

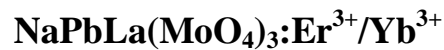
Corresponding author: V.V. Atuchin

Institute of Semiconductor Physics, Novosibirsk 630090, Russia

Phone: +7 (383) 3308889,

E-mail: atuchin@isp.nsc.ru

**Microwave sol-gel synthesis, microstructural and spectroscopic properties of
scheelite-type ternary molybdate upconversion phosphor**



Chang Sung Lim¹, Aleksandr S. Aleksandrovsky^{2,3}, Victor V. Atuchin^{4,5,6,7}, Maxim S.

Molokeev^{8,9,10}, Aleksandr S. Oreshonkov^{9,11}

¹Department of Aerospace Advanced Materials & Chemical Engineering, Hanseo University,
Seosan 356-706, Republic of Korea

²Laboratory of Coherent Optics, Kirensky Institute of Physics Federal Research Center KSC SB
RAS, Krasnoyarsk 660036, Russia

³Department of Photonics and Laser Technologies, Siberian Federal University, Krasnoyarsk
660041, Russia

⁴Laboratory of Optical Materials and Structures, Institute of Semiconductor Physics, SB RAS,
Novosibirsk 630090, Russia

⁵Functional Electronics Laboratory, Tomsk State University, Tomsk 634050, Russia

⁶Laboratory of Single Crystal Growth, South Ural State University, Chelyabinsk 454080, Russia

⁷Research and Development Department, Kemerovo State University, Kemerovo 650000, Russia

⁸Laboratory of Crystal Physics, Kirensky Institute of Physics, Federal Research Center KSC SB
RAS, Krasnoyarsk 660036, Russia

⁹Siberian Federal University, Krasnoyarsk 660041, Russia

¹⁰Department of Physics, Far Eastern State Transport University, Khabarovsk 680021, Russia

¹¹Laboratory of Molecular Spectroscopy, Kirensky Institute of Physics Federal Research Center

KSC SB RAS, Krasnoyarsk 660036, Russia

Abstract

New ternary molybdate $\text{NaPbLa}_{(1-x-y)}(\text{MoO}_4)_3:x\text{Er}^{3+},y\text{Yb}^{3+}$ ($x = y = 0$, $x = 0.05$ and $y = 0.35$, 0.4 , 0.45 and 0.5) phosphors were successfully fabricated by the MSG (microwave sol-gel) method, and the microstructural and spectroscopic properties were characterized. The crystal structure of $\text{NaPbLa}(\text{MoO}_4)_3$ (NPLM) is defined by Rietveld analysis in space group $I4_1/a$ with unit cell parameters $a = 5.3735(2)$ and $c = 11.8668(4)$ Å, $V = 342.65(3)$ Å³, $Z = 4$ ($R_B = 6.64$ %). The unit cell volume of $\text{NaPbLa}(\text{MoO}_4)_3$ (NPLM) is intermediate between those of $\text{NaLa}(\text{MoO}_4)_2$ and PbMoO_4 . Under 980 nm excitation, upconverted yellowish green emission at transitions from ${}^2\text{H}_{11/2}$ and ${}^4\text{S}_{3/2}$ is observed. No concentration quenching in the subsystem of donor ions at the content up to 50 at.% as well as no cross-relaxation losses in the subsystem of acceptor ions at the concentrations as high as 5 at. % is verified. The individual chromaticity points for the samples corresponded to the equal-energy point in the standard CIE diagram.

Key words: Optical materials; Chemical synthesis; Raman spectroscopy; X-ray diffraction;

Phosphors

1. Introduction

For the recent years, complex molybdate crystals have become of extensive interest due to the stable chemical properties, rich crystal chemistry and potential applications in such fields as laser systems, electrochemistry and photonics [1-10]. Complex molybdates are actively investigated as host materials for creation of rare earth doped phosphors appropriate for use in light-emitting devices [1,2,11-15]. Among such crystals, scheelite-type molybdates are widely investigated in

terms of searching new structures, including structure-modulation effects, and promising spectroscopic characteristics [15-19]. One of the most representative scheelite-type molybdates is PbMoO_4 compound, which is suitable for laser application, can be used as a low temperature scintillator crystal and as a working medium in acoustic-optic light modulator [20-22]. In view of the above mentioned properties, it is interesting to investigate effects of Pb ion combining with other cations in scheelite framework. It is known that, in simple molybdates, the scheelite-type structure is comparatively stable and wide size range of big A^{2+} ($\text{A} = \text{Cd-Ba}$) cations can be accommodated without structure disruption [23-25]. However, in binary molybdates, the cation combination appropriate for scheelite-type structure are less clear and only tentative predictions are possible depending on the average big cation size [16,26,27]. In ternary molybdates, the rules governing the scheelite structure stability are unclear.

Recently, new family of ternary molybdate of scheelite-type structure was discovered and efficient up-conversion phosphors were prepared on the base of these hosts [28,29]. The present study is aimed at preparation and evaluation of new ternary molybdate $\text{NaPbLa}(\text{MoO}_4)_4$ (NPLM), where bigger sized Pb^{2+} cation is introduced instead of Ca^{2+} and Sr^{2+} in $\text{NaALa}(\text{MoO}_4)_2$ ($\text{A} = \text{Ca, Sr}$) [30]. The substitution results in bigger average ion radius of cation complex (NaALa) and, respectively, related structural and spectroscopic effects can be considered. Additionally, the $\text{NaPbLa}(\text{MoO}_4)_4:\text{Er}^{3+},\text{Yb}^{3+}$ phosphors will be prepared to estimate the potential of the $\text{NaPbLa}(\text{MoO}_4)_4$ host in optical frequency upconversion (UC) structures.

Among rare-earth ions, the Er^{3+} ion is suitable for the optical frequency conversion via the UC process due to its appropriate configuration of electronic energy levels. The Yb^{3+} ion, commonly used as a sensitizer, can be efficiently excited by IR light source working at ~ 980 nm. Then, the absorbed energy is transferred to the activator ions (Er^{3+}) that drastically increases the emission efficiency. Thus, the $\text{Er}^{3+}/\text{Yb}^{3+}$ co-doping can remarkably enhance the UC efficiency for the shift from infrared to visible light due to the efficiency of the energy transfer from Yb^{3+} to Er^{3+} [31-35]. In the present study, the pure and doped ternary molybdate $\text{NaPbLa}_{(1-x-y)}(\text{MoO}_4)_3:x\text{Er}^{3+},y\text{Yb}^{3+}$

(NPLM: $x\text{Er}^{3+}$, $y\text{Yb}^{3+}$) powder samples with the correct doping concentrations of Er^{3+} and Yb^{3+} ($x = y = 0$, $x = 0.05$ and $y = 0.35, 0.4, 0.45$ and 0.5) were successfully synthesized by the MSG method followed by high-temperature treatment in the air. As it was shown earlier, this method is highly efficient for the preparation of complex molybdate and tungstate compounds for relatively short time [36-39]. The prepared powder samples were characterized by X-ray diffraction (XRD) for Rietveld refinement, scanning electron microscopy (SEM). The Raman and photoluminescence (PL) emission spectra were examined comparatively for different doping levels. The dependence of pump power and Commission Internationale de L'Eclairage (CIE) chromaticity parameters of the UC emission were evaluated in detail.

2. Experimental

In the present experiment, $\text{Na}_2\text{MoO}_4 \cdot 2\text{H}_2\text{O}$, $\text{Pb}(\text{NO}_3)_2$, $\text{La}(\text{NO}_3)_3 \cdot 6\text{H}_2\text{O}$ and $(\text{NH}_4)_6\text{Mo}_7\text{O}_{24} \cdot 4\text{H}_2\text{O}$ in purity of 99.0%, and $\text{Yb}(\text{NO}_3)_3 \cdot 5\text{H}_2\text{O}$ and $\text{Er}(\text{NO}_3)_3 \cdot 5\text{H}_2\text{O}$ in purity of 99.9% were used as received from Sigma-Aldrich, USA. Besides, citric acid in purity of 99.5% was received from Daejung Chemicals, Korea. Distilled water, ethylene glycol (A.R.) and NH_4OH (A.R.) were used to bring the transparent sol formation. As the first step, to prepare the sol of (a) $\text{NaPbLa}(\text{MoO}_4)_3$ (NPLM), $\text{Na}_2\text{MoO}_4 \cdot 2\text{H}_2\text{O}$ for 0.2 mol% and $(\text{NH}_4)_6\text{Mo}_7\text{O}_{24} \cdot 4\text{H}_2\text{O}$ for 0.143 mol% were dissolved in 80 mL 8M NH_4OH with 20 mL ethylene glycol. Subsequently, $\text{Pb}(\text{NO}_3)_2$ for 0.4 mol% and $\text{La}(\text{NO}_3)_3 \cdot 5\text{H}_2\text{O}$ for 0.4 mol% were precisely weighed and dissolved slowly in 100 mL distilled water. Then, the two solutions were mixed together under vigorous stirring and the mixture was adjusted to $\text{pH} = 7-8$ using citric acid and NH_4OH . At this stage, a citric acid molar ratio accounting to numbers of total cation metal ions is adjusted to 2:1. The appropriate amount of the solution, 180-200 mL, was heated up to 80-100°C in a 450 mL Pyrex glass before MSG processing. Consequently, the final solution becomes to be highly transparent.

As to the doped compounds of $\text{NaPbLa}_{(1-x-y)}(\text{MoO}_4)_3 : x\text{Er}^{3+}, y\text{Yb}^{3+}$ ($\text{NPL}_{(1-x-y)}\text{M} : x\text{Er}^{3+}y\text{Yb}^{3+}$), the following variations were made to prepare the solutions for: (b) $\text{NPLa}_{0.6}\text{M} : \text{Er}_{0.05}\text{Yb}_{0.35}$,

La(NO₃)₃·6H₂O for 0.24 mol%, Yb(NO₃)₃·5H₂O for 0.14 mol% and Er(NO₃)₃·5H₂O for 0.02 mol%; (c) NPLa_{0.55}M:Er_{0.05}Yb_{0.4}, La(NO₃)₃·6H₂O for 0.22 mol%, Yb(NO₃)₃·5H₂O for 0.16 mol% and Er(NO₃)₃·5H₂O for 0.02 mol%; (d) NPLa_{0.5}M:Er_{0.05}Yb_{0.45}, La(NO₃)₃·6H₂O for 0.2 mol%, Yb(NO₃)₃·5H₂O for 0.18 mol% and Er(NO₃)₃·5H₂O for 0.02 mol%; and (e) NPLa_{0.45}M:Er_{0.05}Yb_{0.5}, La(NO₃)₃·6H₂O for 0.18 mol%, Yb(NO₃)₃·5H₂O for 0.2 mol% and Er(NO₃)₃·5H₂O for 0.02 mol%.

For the MSG process, a useful microwave oven was utilized at a frequency of 2.45 GHz and maximum output power with 1250 W for 30 min. The mixed solutions were located in the oven under the two kinds of cyclic working steps. At the first step, the MSG process was controlled by the cyclic regime of 40 s on and 20 s off for 15 min. At the second step, the further treatment was continued by the cyclic regime of 30 s on and 30 s off for 15 min. After the MSG process, the sols were treated under ultrasonic radiation for 10 min to bring light yellow colored transparent sols. The transparent sols were dried at 120°C in a dry oven for one week. The obtained black dried gels were ground, heat treated at 350°C for 6 h to evaporate the ethylene glycol and other remained organic substances, and annealed at 850°C for 16 h. As it was previously stated, this temperature range is highly appropriate for calcination of molybdate compounds [3,6,40-42]. After annealing process, pink colored particles were obtained for the doped samples.

The powder diffraction patterns of the new ternary molybdate NPLM:ErYb particles for Rietveld analysis were precisely examined over the range of $2\theta = 5-90^\circ$ at room temperature with a D/MAX 2200 (Rigaku in Japan) diffractometer with Cu-K α radiation and θ - 2θ geometry. The size step of 2θ was 0.02° , and the time counting was 5 s per step. The TOPAS 4.2 package was applied for the Rietveld analysis [43]. The typical microstructure and surface morphology of the obtained particles were observed using SEM (JSM-5600, JEOL in Japan). The PL spectra were relatively recorded using a spectrophotometer (Perkin Elmer LS55 in UK) at room temperature. Pump power dependence of the resultant UC emission intensity was measured at working power from 20 to 110 mW levels. Raman spectra measurements were performed using a LabRam Aramis (Horiba Jobin-Yvon in France) with the spectral resolution of 2 cm^{-1} . The 514.5-nm line of an Ar ion laser was

used as an excitation source; the power on the samples was kept at the 0.5 mW level to avoid the sample decomposition.

3. Results and discussion

The XRD pattern measured for NPLM is shown in Figure 1 and the patterns of doped samples are shown in Figures S1-S4 (Supporting Information). All peaks of powder patterns recorded from $\text{NaPbLa}_{1-x-y}\text{MoO}_4:x\text{Er},y\text{Yb}$ ($x = 0, 0.05$; $y = 0, 0.35, 0.4, 0.45, 0.5$) compounds were successfully indexed by tetragonal cell ($I4_1/a$) with cell parameters close to those of PbMoO_4 [44]. Therefore, the crystal structure of PbMoO_4 was taken as a starting model for Rietveld refinement. The site of Pb^{2+} ion was considered as occupied by Pb, Na, La, Er, Yb ions (Figure 2) with fixed occupations according to suggested formulas. The refinements were stable and gives low R-factors (Table 1, Figures 1, S1-S4). Coordinates of atoms and main bond lengths are summarized in Tables S1 and S2, respectively.

Further details of the crystal structure may be obtained from Fachinformationszentrum Karlsruhe, 76344 Eggenstein-Leopoldshafen, Germany (fax: (+49)7247-808-666; E-mail: crystdata@fiz-karlsruhe.de; http://www.fiz-karlsruhe.de/request_for_deposited_data.html on quoting the deposition numbers: CSD-??????; CSD-??????;...

The dependence of the cell volume on average ion radius of big cations $\text{IR}(\text{Na/Pb/La/Er/Yb})$, excluding Mo^{6+} , in the NPLM:ErYb compounds is shown in Figure 3a. The diagram part containing ternary molybdates can be observed in Figure S5. The IR values were calculated on the base of nominal compositions and known system of ion radii [30]. It is evident that the cell volume linearly decreases with $\text{IR}(\text{Na/Pb/La/Er/Yb})$ decrease or $(x + y)$ increase. This clearly proves the suggested chemical formulas of the solid solutions NPLM:ErYb . Besides, it is very interesting to see the position of NPLM:ErYb compounds among other known scheelite-type molybdates. In Figure 3b, the cell volume of selected simple and complex scheelite-type molybdates is shown as a function of big cation ion radius (IR), where, for complex compounds, the average ion radius of big cations is

calculated on the base of available information [24,28-30,44-50]. The basic curve is generated by simple molybdates with general composition $A^{2+}MoO_4$ ($A = Cd, Ca, Eu, Sr, Ba$) and the drastic unit cell variation by 25% is evident on the A^{2+} cation substitutions. This indicates extremely high stability of the scheelite type structure in reference to the element substitution at the A^{2+} position. The point of the binary scheelite $NaLa(MoO_4)_2$ is not very far from the main line and their structural properties should be governed by the general tendency. Indeed, the addition of $[CaMoO_4]$ block to the composition $NaLa(MoO_4)_2$ results to the formation of scheelite-type compound $NaCaLa(MoO_4)_3$ which cell volume is intermediate between those of $NaLa(MoO_4)_2$ and $CaMoO_4$. The similar trend is observed when the $[PbMoO_4]$ block is added to the composition $NaLa(MoO_4)_2$ with formation of $NaPbLa(MoO_4)_3$, which unit cell volume is intermediate between those of $NaLa(MoO_4)_2$ and $PbMoO_4$. According to this algorithm, the existence of wide family of scheelite-type compounds $NaA^{2+}La(MoO_4)_3$ can be predicted. Within possible cation combinations, the substitution of the $[BaMoO_4]$ block to $NaLa(MoO_4)_3$ is of special interest because, in this case, the particularly big variation of the unit cell volume can be assumed in reference to that of $NaLa(MoO_4)_3$. Above this, the existence of $NaA^{2+}Ln(MoO_4)_3$ ($Ln =$ rare earth elements) compounds is also supposed that promises for use of the $NaA^{2+}Ln(MoO_4)_3$ hosts in photonics because wide range rare earth element substitution is possible at the Ln position without structure destruction and drastic defect generation.

The SEM images obtained for the representative compositions (a) NPLM and (b) $NPLM:0.05Er^{3+},0.5Yb^{3+}$ are shown in Fig. 4. Both the samples contain closely packed grains 10-25 μm in size. The grain micromorphology in both samples is very similar. This means that the rare-earth ion substitution at the La^{3+} sites in NPLM has no influence in the micromorphology.

The Raman spectrum of the synthesized $NaPbLa(MoO_4)_3$ is shown in Fig. 5. It can be divided into three sets of Raman bands: 950–700, 425–275 and 275–100 cm^{-1} . The Raman modes in high wavenumber region refer to Mo–O symmetric and antisymmetric stretching vibrations of the MoO_4^{2-} tetrahedra. The modes in middle frequency region are assigned to O–Mo–O symmetric and

antisymmetric bending modes of the MoO_4^{2-} tetrahedra, and the Raman lines in low wavenumber region correspond to translations and librations of MoO_4^{2-} tetrahedra and Na/Pb/La ions.

In Table 2, the correlation between the free MoO_4^{2-} ion, site symmetry and factor group symmetry of unit cell is shown. The vibrational representation for the tetragonal unit cell of NPLM at Brillouin zone center is given by the following equation: $\Gamma_{\text{vibr}} = 3A_g + 7A_u + 7B_g + 3B_u + 14E_g + 14E_u$. According to the selection rules, the A_g , B_g and E_g modes are Raman active, A_u and E_u are IR active, and B_u modes are silent. Thus, three Raman bands should be observed in the region of stretching vibrations and four bands in the region of bending vibrations of MoO_4 tetrahedra. The strong Raman band at 881.2 cm^{-1} (A_g) is assigned to the ν_1 vibrational mode of MoO_4^{2-} ion, and bands at 818.6 (B_g) and 757.3 cm^{-1} (E_g) are assigned to the ν_3 vibrational modes of MoO_4^{2-} ion. The bands at 380.1 (B_g) and 366.9 cm^{-1} (E_g) are the ν_4 vibrational modes of MoO_4^{2-} ion, and bands at 326.4 (B_g) and 319.0 cm^{-1} (A_g) are the ν_2 vibrational modes of MoO_4^{2-} ion. The deconvolution of experimental Raman spectrum by fitting with use of Lorentzian function revealed an extra bands at 900.4 , 795.1 , 668.3 and 292.6 cm^{-1} . The appearance of these lines can be explained as local distortions of MoO_4 tetrahedra caused by influence of Na/Pb/La ions. The wide band at 230.6 cm^{-1} is assigned to the rotation of MoO_4^{2-} ions. The other bands in low-wavenumber region of Raman spectrum are external modes (translations of MoO_4^{2-} and Na/Pb/La ions and their mixed vibrations).

In the case of $\text{NaPbLa}(\text{MoO}_4)_3$ doped with Er^{3+} and Yb^{3+} ions the Raman spectra are totally covered with the luminescence signal of Er^{3+} ions, as shown in Figure 6. Only the very small peak at 881.2 cm^{-1} related to symmetric stretching vibration of MoO_4 tetrahedra can be distinguished in the spectra. It should be noted, that an increasing of the Yb^{3+} content leads to the difference of Er^{3+} ${}^2\text{H}_{11/2}$ multiplet intensity. This fact can be explained in the framework of different local structure of Er^{3+} , as induced by Yb^{3+} doping level variation (Table S2).

UC luminescence spectra of NPLM coactivated by 5% of Er^{3+} ions and increasing content of Yb^{3+} ions measured at room temperature under 980 nm excitation are presented in Fig. 7. Upconverted emission in the green at the transition from ${}^4\text{H}_{11/2}$ state to ${}^4\text{I}_{15/2}$ ground state is

prevailing over the emission at the transition from $^4S_{3/2}$ to $^4H_{15/2}$, while deep red emission at the transition from $^4F_{9/2}$ to $^4H_{15/2}$ is approximately 25 times weaker in all samples as compared to the green emission. Increase of Yb content from 35 to 50% results in continuous growth of UC emission at all lines indicating the absence of concentration quenching in the subsystem of Yb ions up to the doping level as high as 50%. Power dependences of UCL show slopes with $n < 2$ that indicates the absence of cross-relaxation in the system of Er ions at the concentration as high as 5%. The features specified above must be ascribed to the advantages of molybdate crystalline matrix used.

The CIE diagram and chromaticity coordinates (x , y) of the $\text{NaPbLa}(\text{MoO}_4)_3:\text{Er}^{3+}, \text{Yb}^{3+}$ phosphors are shown in Fig. 8. The individual chromaticity points of CIE for the samples (a), (b), (c) and (d) are exhibited by the legend in Fig. 8(A). The calculated values for chromaticity coordinates are $x = 0.237$ and $y = 0.669$ for (a), $x = 0.246$ and $y = 0.640$ for (b), $x = 0.248$ and $y = 0.610$ for (c), and $x = 0.269$, and $y = 0.529$ for (d), corresponding to the equal-energy point in the standard CIE diagram. As it is seen, the $\text{NaPbLa}(\text{MoO}_4)_3:\text{Er}^{3+}, \text{Yb}^{3+}$ phosphors provides emission in the yellowish green region.

4. Conclusions

New ternary molybdate $\text{NPLM}:\text{Er}^{3+}, \text{Yb}^{3+}$ phosphors were successfully synthesized by MSG, and the microstructural and spectroscopic properties were investigated in detail. The general dependence of unit cell on the average ion radii of all cations, excluding Mo^{6+} , in the scheelite type molybdates is defined with use of available experimental data on the crystal structures. The unit cell volume of NPLM is intermediate between those of $\text{NaLa}(\text{MoO}_4)_2$ and PbMoO_4 . The diagram provides predictions of the existence of wide family of scheelite-type compounds $\text{NaA}^{2+}\text{La}(\text{MoO}_4)_3$ ($A = \text{Cd-Ba}$) with great potential for creation new phosphor materials. The rare-earth ion substitution at the La^{3+} sites in NPLM has no influence in the micromorphology variation. The Raman spectra of NPLM doped with Er^{3+} and Yb^{3+} ions were totally covered with the luminescence

signal of Er^{3+} ions, and increasing of the Yb^{3+} content resulted to the difference of $\text{Er}^{3+} \ ^2\text{H}_{11/2}$ multiplet intensity. The chromaticity coordinates (x , y) values for the samples indicated in reference to the equal-energy point in the standard CIE diagram. The crystalline matrix under investigation favors domination of yellowish-green upconverted emission of Er ions and enables absence of concentration quenching up to Yb content as high as 50% as well as the absence of cross-relaxation at Er content as high as 5%.

Acknowledgements

This research was supported by the Basic Science Research Program through the National Research Foundation of Korea(NRF) funded by the Ministry of Science, ICT and future Planning (2018R1D1A1A09082321). The authors are grateful for the support from RFBR (16-52-48010, 18-32-20011). The work was supported by Act 211 Government of the Russian Federation, contract № 02.A03.21.0011. Additionally the work was partially supported by the Ministry of Science and Higher Education of the Russian Federation (4.1346.2017/4.6).

References

1. Katrien W. Meert, Vladimir A. Morozov, Artem M. Abakumov, Joke Hadermann, Dirk Poelman, Philippe F. Smet, Energy transfer in Eu³⁺ doped scheelites: use as thermographic phosphor, *Opt. Exp.* 22 (2014) A961-A972.
2. Pinglu Shi, Zhiguo Xia, Maxim. S. Molokeev, Victor V. Atuchin, Crystal chemistry and luminescence properties of red-emitting CsGd_{1-x}Eu_x(MoO₄)₂ solid-solution phosphors, *Dalton Trans.* 43 (2014) 9669-9676.
3. A.A. Savina, V.V. Atuchin, S.F. Solodovnikov, Z.A. Solodovnikova, A.S. Krylov, E.A. Maksimovsky, M.S. Molokeev, A.S. Oreshonkov, A.M. Pugachev, E.G. Khaikina, Synthesis, structural and spectroscopic properties of acentric triple molybdate Cs₂NaBi(MoO₄)₂, *J. Solid State Chem.* 225 (2015) 53-58.
4. Sergei Kurilchik, Pavel Loiko, Anatol Yasukevich, Vyacheslav Trifonov, Anna Volokitina, Elena Vilejshikova, Viktor Kisel, Xavier Mateos, Aleksander Baranov, Oleg Goriev, Nikolay Kuleshov, Anatoly Pavlyuk, Orthorombic Yb:Li₂Zn₂(MoO₄)₃ – a novel potential crystal for broadly tunable lasers, *Laser Phys. Lett.* 14 (2017) 085804.
5. Aleksandra A. Savina, Vladimir A. Morozov, Anton L. Buzlukov, Irina Yu. Arapova, Sergey Yu. Stefanovich, Yana V. Baklanova, Tatiana A. Denisova, Nadezhda I. Medvedeva, Michel Bardet, Joke Hadermann, Bogdan I. Lazoryak, Elena G. Khaikina, New solid electrolyte Na₉Al(MoO₄)₆: Structure and Na⁺ ion conductivity, *Chem. Mater.* 29 (2017) 8901-8913.
6. Sergey F. Solodovnikov, Victor V. Atuchin, Zoya A. Solodovnikova, Oleg Y. Khyzhun, Mykola I. Danylenko, Denis P. Pishchur, Pavel E. Plyusnin, Alexey M. Pugachev, Tatiana A. Gavrilova, Alexander P. Yelisseyev, Ali H. Reshak, Zeyad A. Alahmed, Nadir F. Habubi, Synthesis, structural, thermal, and electronic properties of palmierite-related double molybdate α -Cs₂Pb(MoO₄)₂, *Inorg. Chem.* 56 (6) (2017) 3276-3286.
7. Shriya Sinha, Kaushal Kumar, Studies on up/down-conversion emission of Yb³⁺ sensitized Er³⁺ doped MLa₂(MoO₄)₄ (M = Ba, Sr and Ca) phosphors for thermometry and optical heating, *Opt.*

Mater. 75 (2018) 770-780.

8. Pavel Loiko, Esrom Kifle, Josef Maria Serres, Xavier Mateos, Magdalena Aguiló, Francesc Diaz, Elena Vilejshikova, Nikolai Kuleshov, Anatoly Pavlyuk, Efficient continuous-wave in-band pumped Nd:KY(MoO₄)₂ laser.
9. Victor V. Atuchin, Aleksandr S. Aleksandrovsky, Bair G. Bazarov, Jibzema G. Bazarova, Olga D. Chimitova, Yuriy G. Denisenko, Tatyana A. Gavrilova, Alexander S. Krylov, Eugene A. Maximovskiy, Maxim. S. Molokeev, Aleksandr S. Oreshonkov, Alexey M. Pugachev, Nikolay V. Surovtsev, Exploration of structural, vibrational and spectroscopic properties of self-activated orthorhombic double molybdate RbEu(MoO₄)₂ with isolated MoO₄ units, J. Alloys Compd. 785 (2019) 692-697.
10. Nadezhda I. Medvedeva, Anton L. Buzlukov, Alexander V. Skachkov, Alexandra A. Savina, Vladimir A. Morozov, Yana V. Baklanova, Irina E. Animitsa, Elena G. Khaikina, Tatiana A. Denisova, Sergei F. Solodovnikov, Mechanism of sodium ion diffusion in alluaudite-type Na₅Sc(MoO₄)₄ from NMR experiment and ab initio calculations, J. Phys. Chem. C (2019) DOI: 10.1021/acs.jpcc.8b11654.
11. Jiayue Sun, Yujing Lan, Zhiguo Xia, Haiyan Du, Sol-gel synthesis and green upconversion luminescence in BaGd₂(MoO₄)₄:Yb³⁺,Er³⁺ phosphors, Opt. Mater. 33 (2011) 576-581.
12. P.S. Dutta, A. Kumar, Eu³⁺ activated molybdate and tungstate based red phosphors with charge transfer band in blue region, ECS J. Solid State Sci. Technol. 2 (2) (2013) R3153-3167.
13. Chang Sung Lim, Aleksandr Aleksandrovsky, Maxim Molokeev, Aleksandr Oreshonkov, Victor Atuchin, The modulated structure and frequency upconversion properties of CaLa₂(MoO₄)₄:Ho³⁺/Yb³⁺ phosphors prepared by microwave synthesis, Phys. Chem. Chem. Phys. 17 (2015) 19278-19287.
14. Yiru Wang, Xiaohua Liu, Lindan Jing, Pengfei Niu, Tunable white light and energy transfer of Dy³⁺ and Eu³⁺ doped Y₂Mo₄O₁₅ phosphors, Ceram. Int. 42 (2016) 13004-13010.
15. Heng Wang, Ting Yang, Li Feng, Zhanglei Ning, Mengjiao Liu, Xin Lai, Daojiang Gao, Jian Bi,

- Energy transfer and multicolor tunable luminescence properties of $\text{NaGd}_{0.5}\text{Tb}_{0.5-x}\text{Eu}_x(\text{MoO}_4)_2$ phosphors for UV-LED, *J. Elect. Mater.* 47 (11) (2018) 6494-6506.
16. Olga D. Chimitova, Victor V. Atuchin, Baig G, Bazarov, Maxim S. Molokeev, Zhibzema G. Bazarova, The formation and structural parameters of new double molybdates $\text{RbLn}(\text{MoO}_4)_2$ ($\text{Ln} = \text{Pr}, \text{Nd}, \text{Sm}, \text{Eu}$), *Proc. SPIE* 8771 (2013) 877711A.
 17. Artem A. Abakumov, Vladimir A. Morozov, Alexander A. Tsirlin, Johan Verbeeck, Joke Hadermann, Cation ordering and flexibility of the BO_4^{2-} tetrahedra in incommensurately modulated $\text{CaEu}_2(\text{BO}_4)_4$ ($\text{B} = \text{Mo}, \text{W}$) scheelites, *Inorg. Chem.* 53 (2014) 9407-9415.
 18. Rajagopalan Krishnan, Jagannathan Thirumalai, Venkatakrishnan Mahalingam, Srinivas Mantha, Manthramoorthy Lavanya, Synthesis, luminescence and photometric characteristics of $\text{Ca}_{0.5}\text{La}(\text{MoO}_4)_2:\text{Ln}^{3+}$ ($\text{Ln} = \text{Eu}, \text{Tb}, \text{Dy}$) phosphors, *Mater. Chem. Phys.* 162 (2015) 41-49.
 19. J.V.B. Moura, G.S. Pinheiro, J.V. Silveira, P.T.C. Freire, B.C. Viana, C. Luz-Lima, $\text{NaCe}(\text{MoO}_4)_2$ microcrystals: Hydrothermal synthesis, characterization and photocatalytic performance, *J. Phys. Chem. Solids* 111 (2017) 258-265.
 20. L.F. Johnson, Optical maser characteristics of rare-earth ions in crystals. *J. Appl. Phys.* 34 (4),(1963) 897-909.
 21. M. Minowa, K. Itakura, S. Moriyama, W. Ootani, Measurement of the property of cooled lead molybdate as a scintillator, *Nucl. Instrum. Meth. Phys. Res.* 320 (3) (1992) 500-503.
 22. S. Takano, S. Esashi, K. Mori, T. Namikata, Growth of high-quality single crystals of lead molybdate, *J. Cryst. Growth* 24 (1974) 437-440.
 23. E. Guermen, E. Daniels, J.S. King, Crystal structure refinement of SrMoO_4 , SrWO_4 , CaMoO_4 , and BaWO_4 by neutron diffraction, *J. Chem. Phys.* 55 (1971) 1093-1097.
 24. M. Daturi, G. Busca, M.M. Borel, A. Leklaire, P. Piaggio, Vibrational and XRD study of the system CdWO_4 - CdMoO_4 , *J. Solid State Chem.* 101 (1997) 4358-4369.
 25. V. Nassif, R.E. Carbonio, J.A. Alonso, Neutron diffraction study of the crystal structure of BaMoO_4 : a suitable precursor for metallic BaMoO_3 perovskite, *J. Solid State Chem.* 146 (1999)

266-270.

26. V.V. Atuchin, O.D. Chimitova, T.A. Gavrilova, M.S. Molocheev, Sung-Jin Kim, N.V. Surovtsev, B.G. Bazarov, Synthesis, structural and vibrational properties of microcrystalline $\text{RbNd}(\text{MoO}_4)_2$, *J. Cryst. Growth* 318 (2011) 683-686.
27. V.V. Atuchin, O.D. Chimitova, S.V. Adichtchev, J.G. Bazarov, T.A. Gavrilova, M.S. Molocheev, N.V. Surovtsev, Zh.G. Bazarova, Synthesis, structural and vibrational properties of microcrystalline $\text{RbSm}(\text{MoO}_4)_2$, *Mater. Lett.* 106 (2013) 26-29.
28. Chang Sung Lim, Aleksandr S. Aleksandrovsky, Maxim. S. Molocheev, Aleksandr S. Oreshonkov, Denis A. Ikonnikov, Victor V. Atuchin, Triple molybdate scheelite-type upconversion phosphor $\text{NaCaLa}(\text{MoO}_4)_3:\text{Er}^{3+}/\text{Yb}^{3+}$: structural and spectroscopic properties, *Dalton Trans.* 45 (2016) 15541-15551.
29. Chang Sung Lim, Aleksandr S. Aleksandrovsky, Maxim. S. Molocheev, Aleksandr S. Oreshonkov, Denis A. Ikonnikov, Victor V. Atuchin, Microwave synthesis and spectroscopic properties of ternary scheelite-type molybdate phosphors $\text{NaSrLa}(\text{MoO}_4)_2:\text{Er}^{3+},\text{Yb}^{3+}$, *J. Alloys Compd.* 713 (2017) 156-163.
30. R.D. Shannon, Revised effective ionic radii and systematic studies of interatomic distances in halides and chalcogenides, *Acta Cryst. A* 32 (1976) 751-767.
31. Jing Zhou, Qian Liu, Wei Feng, Yun Sun, Fuyou Li, Upconversion luminescent materials: Advances and applications, *Chem. Rev.* 115 (1) (2015) 395-465.
32. Chang Sung Lim, Aleksandr Aleksandrovsky, Maxim Molocheev, Aleksandr Oreshonkov, Victor Atuchin, Microwave sol-gel synthesis and upconversion photoluminescence properties of $\text{CaGd}_2(\text{WO}_4)_4:\text{Er}^{3+}/\text{Yb}^{3+}$ phosphors, *J. Solid State Chem.* 228 (2015) 160-166.
33. Fangrui Cheng, Zhiguo Xia, Xiping Jing, Ziyuan Wang, Li/Ag ratio dependent structure and upconversion photoluminescence of $\text{Li}_x\text{Ag}_{1-x}\text{Yb}_{0.99}(\text{MoO}_4)_2:0.01\text{Er}^{3+}$ phosphors, *Phys. Chem. Chem. Phys.* 17 (2015) 3689-3696.
34. Chang Sung Lim, Victor Atuchin, Aleksandr Aleksandrovsky, Maxim Molocheev, Aleksandr

- Oreshonkov, Microwave sol-gel synthesis of $\text{CaGd}_2(\text{MoO}_4)_4:\text{Er}^{3+}/\text{Yb}^{3+}$ phosphors and their upconversion photoluminescence properties, *J. Am. Ceram. Soc.* 98 (10) (2015) 3223-3230.
35. Ming-Jun Song, Yan Zhang, Na-Na Zhang, Lin-Tong Wang, Qin-Guo Meng, Up-conversion properties of $\text{Er}^{3+}/\text{Yb}^{3+}$ co-doped $\text{Li}_3\text{Ba}_2\text{Gd}_3(\text{MoO}_4)_8$ phosphors, *Chin. J. Struct. Chem.* 37 (2) (2018) 210-218.
36. Kirill I. Rybakov, Eugene A. Olevsky, Ekaterina V. Krikun, Microwave sintering: Fundamentals and modeling, *J. Am. Ceram. Soc.* 96 (4) (2013) 1003-1020.
37. Helen J. Kitchen, Simon R. Vallance, Jennifer L. Kennedy, Nuria Tapia-Ruiz, Lucia Carassiti, Andrew Harrison, A. Gavin Whittaker, Timothy D. Drysdale, Samuel W. Kingman, Duncan H. Gregory, Modern microwave methods in solid-state inorganic materials chemistry: From fundamentals to manufacturing, *Chem. Rev.* 114 (2014) 1170-1206.
38. Jeong Ho Ryu, Sang-Mo Koo, Dong Suk Chang, Jong-Won Yoon, Chang Sung Lim, Kwang Bo Shim, Microwave-assisted synthesis of PbWO_4 nano-powders via a citrate complex precursor and its photoluminescence, *Ceram. Int.* 32 (2006) 647-652.
39. Chang Sung Lim, Upconversion photoluminescence properties of $\text{SrY}_2(\text{MoO}_4)_4:\text{Er}^{3+}/\text{Yb}^{3+}$ phosphors synthesized by a cyclic microwave-modified sol-gel method, *Infrared Phys. Tech.* 67 (2014) 371-376.
40. V.V. Atuchin, V.G. Grossman, S.V. Adichtchev, N.V. Surovtsev, T.A. Gavrilova, B.G. Bazarov, Structural and vibrational properties of microcrystalline $\text{TlM}(\text{MoO}_4)_2$ ($\text{M} = \text{Nd}, \text{Pr}$) molybdates, *Opt. Mater.* 34 (2012) 812-816.
41. Tao Wu, Yunfei Liu, Yinong Lu, Ling Wei, Hong Gao, Hu Chen, Morphology-controlled synthesis, characterization, and luminescence properties of $\text{KEu}(\text{MoO}_4)_2$ microcrystals, *CrystEngComm* 15 (2013) 2761-2768.
42. V.V. Atuchin, A.S. Aleksandrovsky, O.D. Chimitova, T.A. Gavrilova, A.S. Krylov, M.S. Molokeev, A.S. Oreshonkov, B.G. Bazarov, J.G. Bazarova, Synthesis and spectroscopic properties of monoclinic $\alpha\text{-Eu}_2(\text{MoO}_4)_3$, *J. Phys. Chem. C* 118 (28) (2014) 15404-15411.

43. Bruker AXS TOPAS V4: General profile and structure analysis software for powder diffraction data. – User’s Manual. Bruker AXS, Karlsruhe, Germany. 2008.
44. C. Lugli, L. Medici, D. Saccardo, Natural wulfenite: structural refinement by single-crystal X-ray diffraction, *Neues Jahrb. Mineral. Monatsh.* (6) (1999) 281-288.
45. T.I. Bylichki, L.I. Soleva, E.A. Pobedims, N.A. Poraikos, N.V. Belov, Crystal structures of Ba molybdate and Ba tungstate, *Soviet Physics Crystallography*, USSR 15 (1) (1970) 130.
46. I.C. Nogueira, L.S. Cavalcante, P.F.S. Pereira, M.M. De Jesus, J.M. Rivas Mercury, N.C. Batista, M. Siu Li, E. Longo, Rietveld refinement, morphology and optical properties of $(\text{Ba}_{1-x}\text{Sr}_x)\text{MoO}_4$ crystals, *J. Appl. Cryst.* 46 (5) (2013) 1434-1446.
47. P. Gall, P. Gougeon, The scheelite-type europium molybdate $\text{Eu}_{0.96}\text{MoO}_4$, *Acta Cryst. E* 62 (5) (2006) i120-i121.
48. Raymond G. Teller, Refinement of some $\text{Na}_{0.5-x}\text{M}'_{0.5+x/3}\square_{2x/3}\text{MoO}_4$, $\text{M}' = \text{Bi}, \text{Ce}, \text{La}$, scheelite structures with powder neutron and X-ray diffraction data, *Acta Cryst. C* 48 (12) (1992) 2101-2104.
49. R.M. Hazen, L.W. Finger, J.W. Mariathasan, High-pressure crystal chemistry of scheelite-type tungstates and molybdates, *J. Phys. Chem. Solids* 46 (2) (1985) 253-263.
50. Chang Sung Lim, Microwave sol-gel derived $\text{NaCaGd}(\text{MoO}_4)_3:\text{Er}^{3+}/\text{Yb}^{3+}$ phosphors and their upconversion photoluminescence properties, *Infrared Phys. Technol.* 76 (2016) 353-359.
51. K. Nakamoto, *Infrared and Raman spectra of inorganic and coordination compounds*, 6th edn. Wiley, New York etc., 2009.

Table 1. Main parameters of processing and refinement of the NPLM: $x\text{Er}^{3+},y\text{Yb}^{3+}$ samples

Compound	x, y	Space group	Z	Cell parameters (\AA), cell volume (\AA^3)	R_p, R_B (%), χ^2
NPLM	0, 0	$I4_1/a$	4	$a = 5.3735$ (2) $c = 11.8668$ (4) $V = 342.65$ (3)	14.16, 6.64 1.30
NPLM: 0.05Er,0.35Yb	0.05, 0.35	$I4_1/a$	4	$a = 5.3301$ (4) $c = 11.756$ (1) $V = 333.99$ (6)	13.14, 4.52 1.31
NPLM: 0.05Er,0.4Yb	0.05, 0.4	$I4_1/a$	4	$a = 5.3208$ (2) $c = 11.7284$ (5) $V = 332.04$ (3)	12.95, 4.85 1.35
NPLM: 0.05Er,0.45Yb	0.05, 0.45	$I4_1/a$	4	$a = 5.3150$ (2) $c = 11.7189$ (7) $V = 331.06$ (4)	11.66, 2.63 1.23
NPLM: 0.05Er,0.5Yb	0.05, 0.5	$I4_1/a$	4	$a = 5.3099$ (2) $c = 11.7010$ (5) $V = 329.91$ (2)	10.91, 2.49 1.11

Table 2. Correlation diagram between T_d point symmetry, S_4 site symmetry and C_{4h} factor group symmetry for MoO_4 tetrahedra

Wavenumber, cm^{-1} [51]	T_d Point group	S_4 Site symmetry	C_{4h} Factor group symmetry
897	$A_1(\nu_1)$	A	A_g+B_u
317	$E(\nu_2)$	$A+B$	$A_g+B_u+B_g+A_u$
837	$F_2(\nu_3)$	$B+\{^2E, ^1E\}$	$B_g+A_u+E_g+E_u$
-	$F_2(\nu_4)$	$B+\{^2E, ^1E\}$	$B_g+A_u+E_g+E_u$

Captions

Fig. 1. The difference Rietveld plot of NPLM.

Fig. 2. The crystal structure of NPLM. The unit cell is outlined. The lone atoms are omitted for clarity.

Fig. 3. (a) Dependence of cell volume on averaged ion radii $IR(\text{Na/Pb/La/Er/Yb})$ of NPLM: $x\text{Er}^{3+},y\text{Yb}^{3+}$ and (b) the NPLM: $x\text{Er}^{3+},y\text{Yb}^{3+}$ crystals among other representative scheelite-type molybdates.

Fig. 4. Scanning electron microscopy images of the synthesized (a) NPLM and (b) NPLM:0.05Er³⁺,0.5Yb³⁺ particles.

Fig. 5. Raman spectrum of NPLM powder. The fit was done using the Lorentzian function.

Fig. 6. Luminescence from $^2\text{H}_{11/2}$ and $^4\text{S}_{3/2}$ multiples of the Er^{3+} ions normalized to most intensive band of $^4\text{S}_{2/3}$ multiplet in the region of lattice vibrations of NPLM: $x\text{Er},y\text{Yb}$.

Fig. 7. The UC photoluminescence spectra of (a) NPLM:0.05Er,0.35Yb, (b) NPLM:0.05Er,0.40Yb, (c) NPLM:0.05Er,0.45Yb, and (d) NPLM:0.05Er,0.50Yb particles excited under 980 nm at room temperature.

Fig. 8. The logarithmic scale dependence of the UC emission intensity on the pump power in the range from 20 to 110 mW at 525, 550 and 655 nm in the NPLM:0.05Er³⁺,0.35Yb³⁺ sample.

Fig. 9. (A) CIE chromaticity diagram for the NPLM: $x\text{Er}^{3+}$, $y\text{Yb}^{3+}$ phosphors, and (B) calculated chromaticity coordinates (x, y) values. The emission points for the sample (a) NPLM:0.05Er³⁺,0.35Yb³⁺, (b) NPLM:0.05Er³⁺,0.40Yb³⁺, (c) NPLM:0.05Er³⁺,0.45Yb³⁺, and (d) NPLM:0.05Er³⁺,0.50Yb³⁺ particles are shown in the legend.

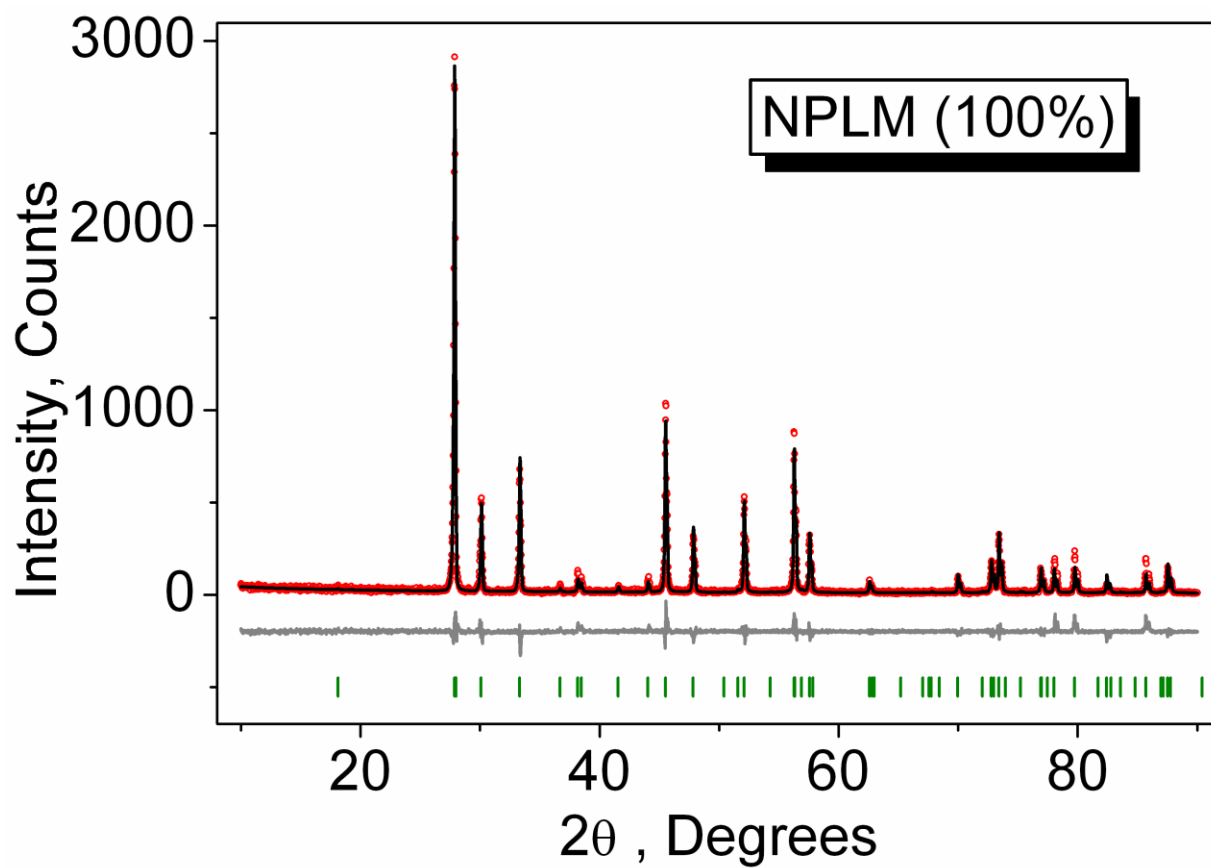


Fig. 1.

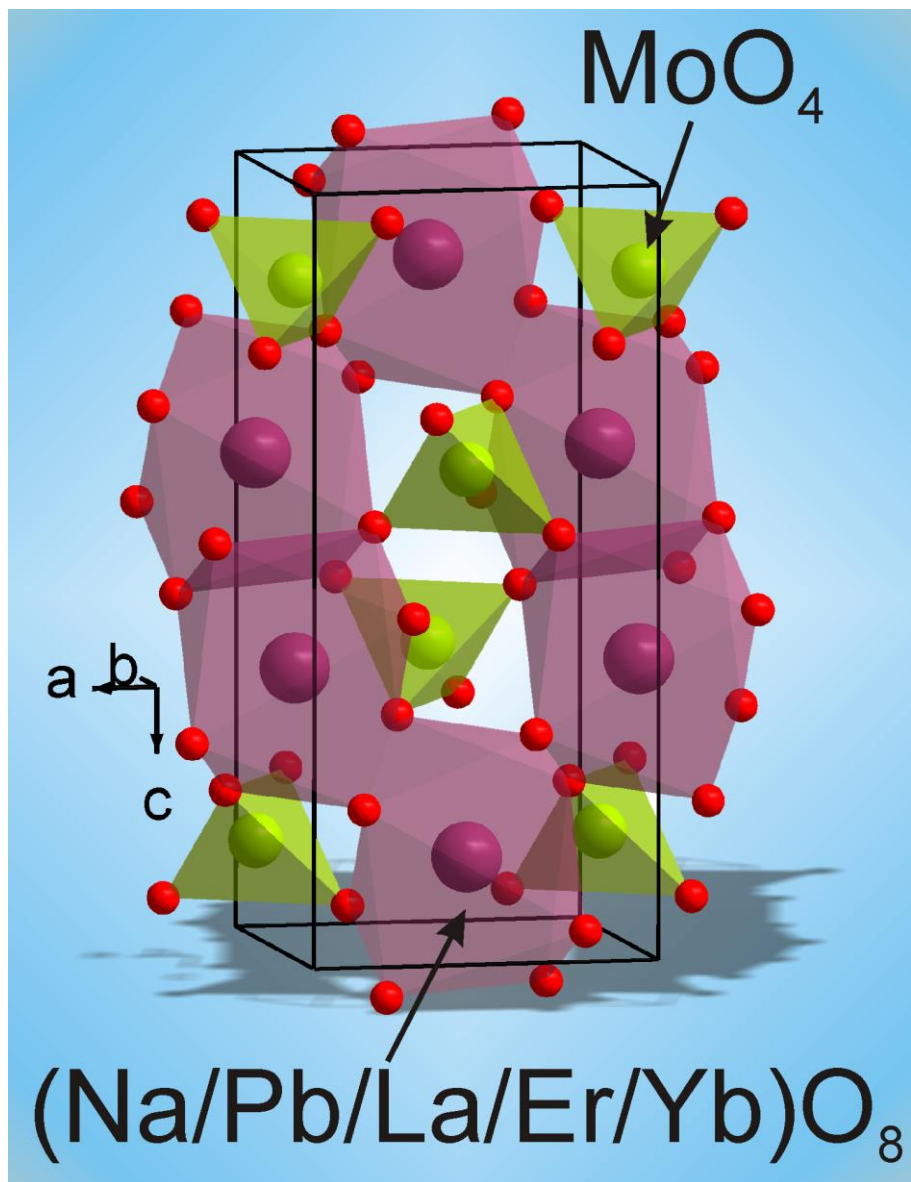
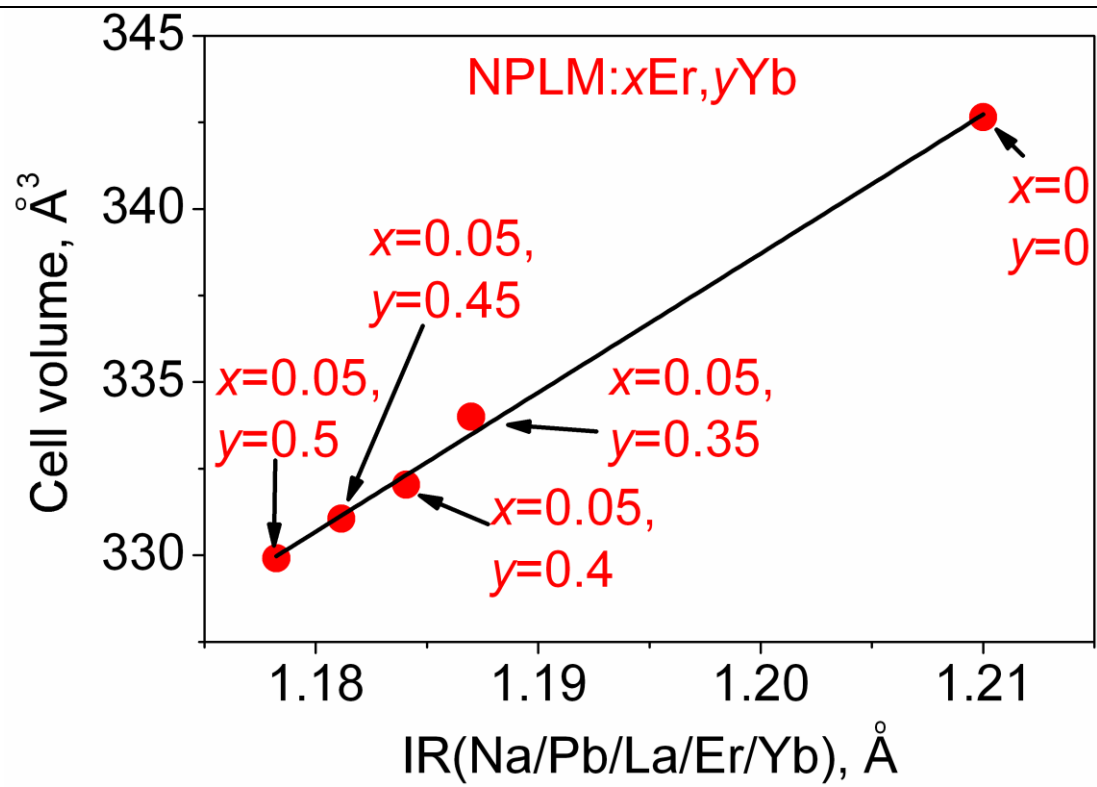
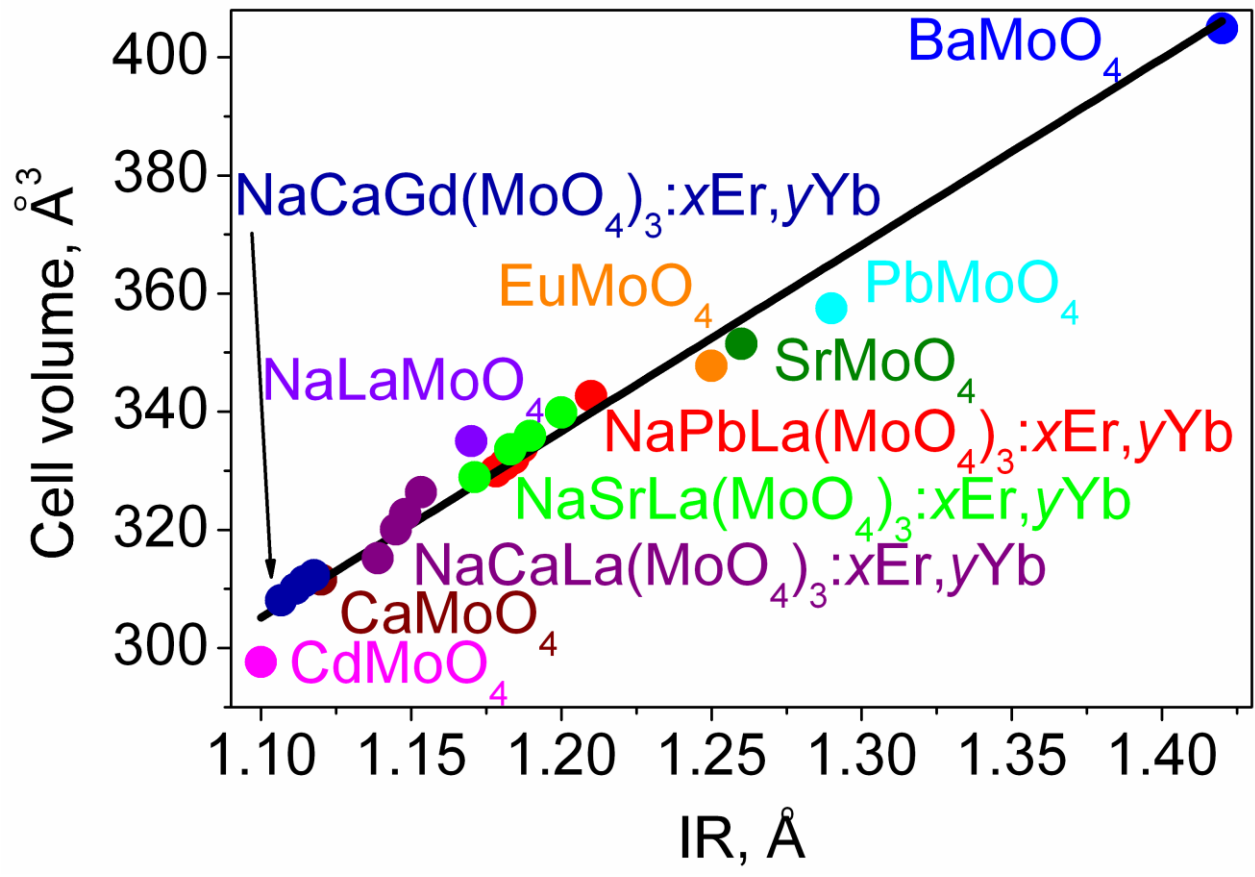


Fig. 2.

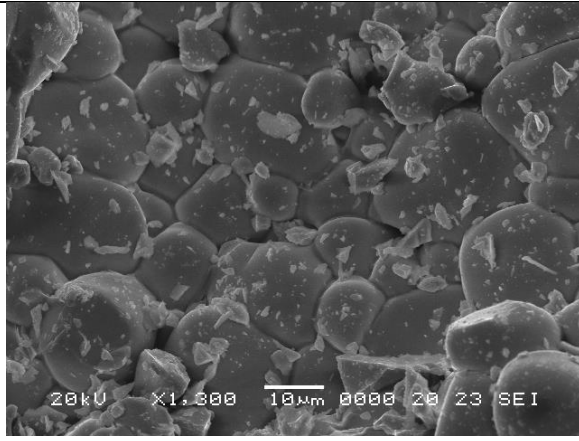


a

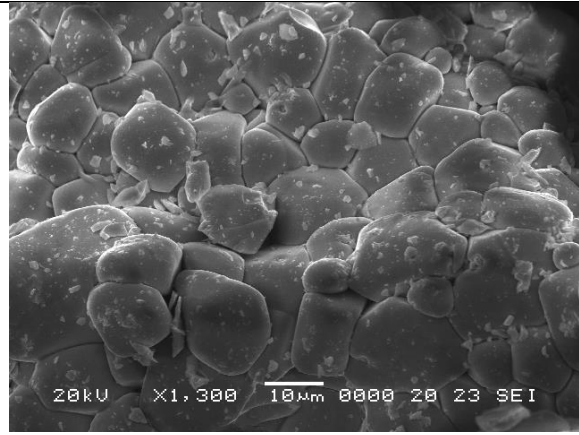


b

Fig. 3.



(a)



(b)

Fig. 4.

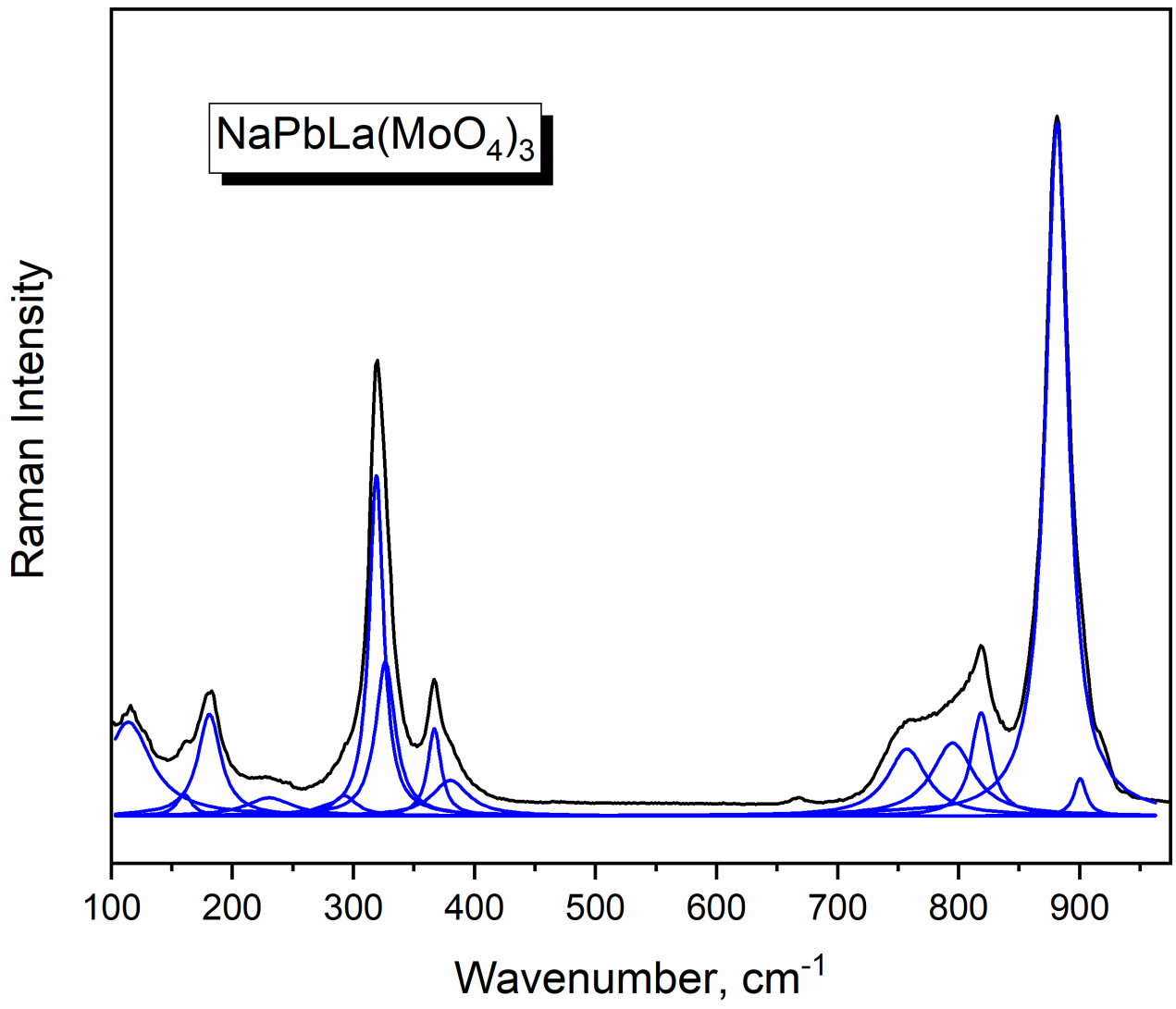


Fig. 5.

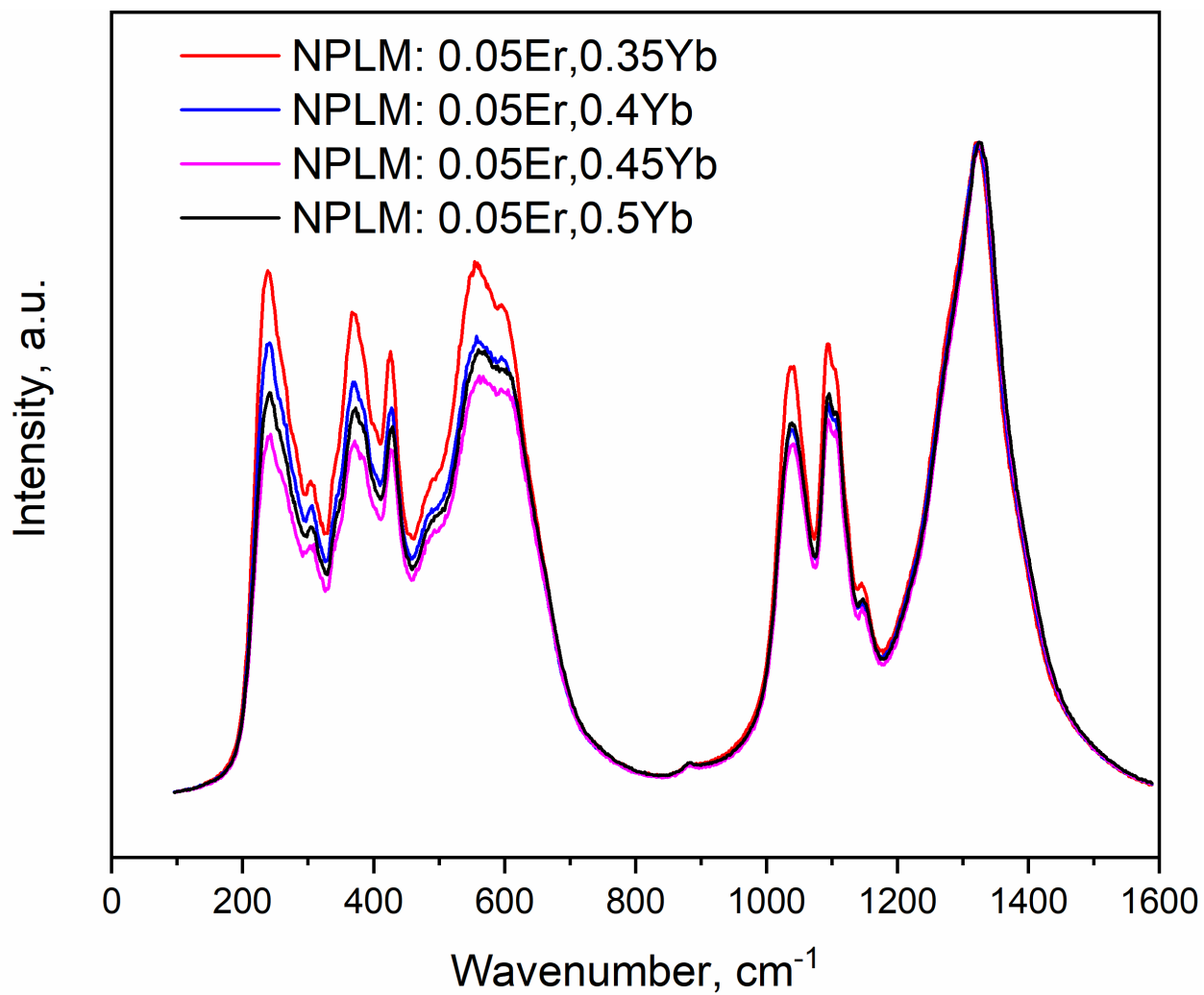


Fig. 6.

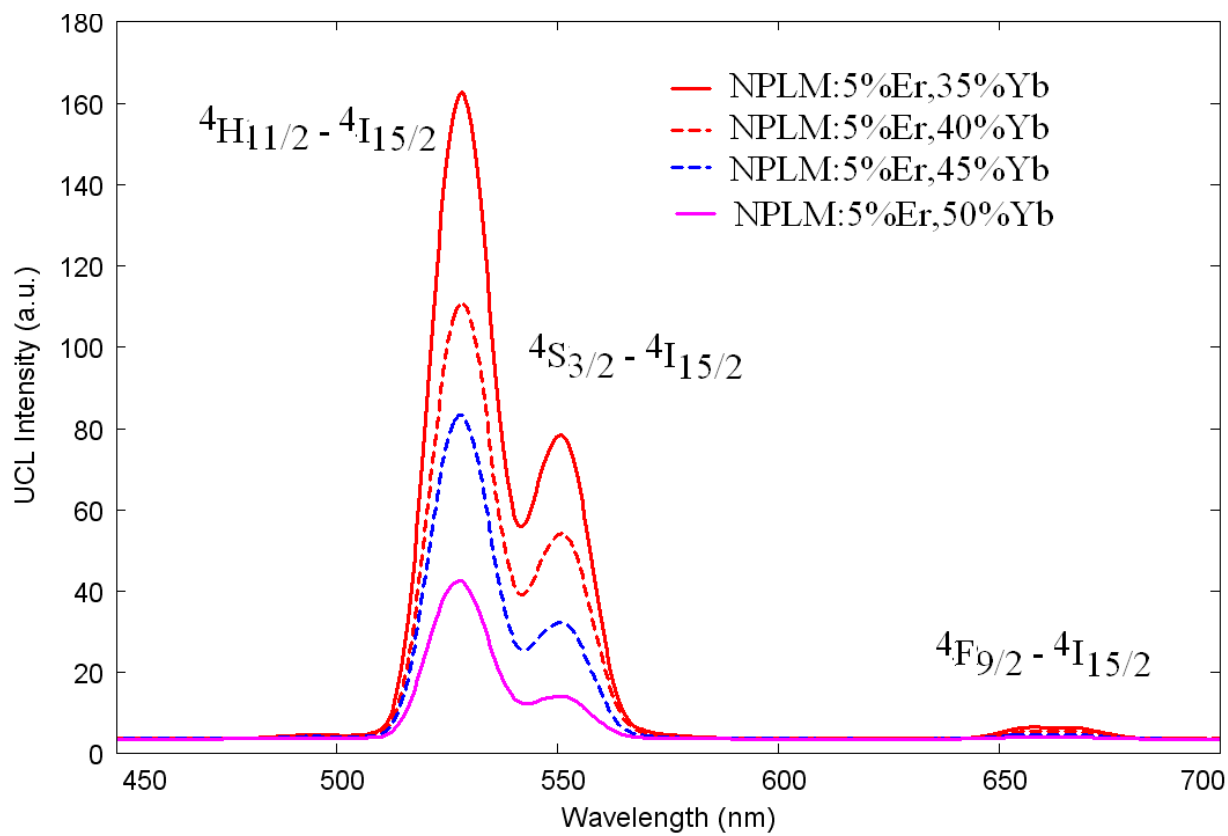


Fig. 7.

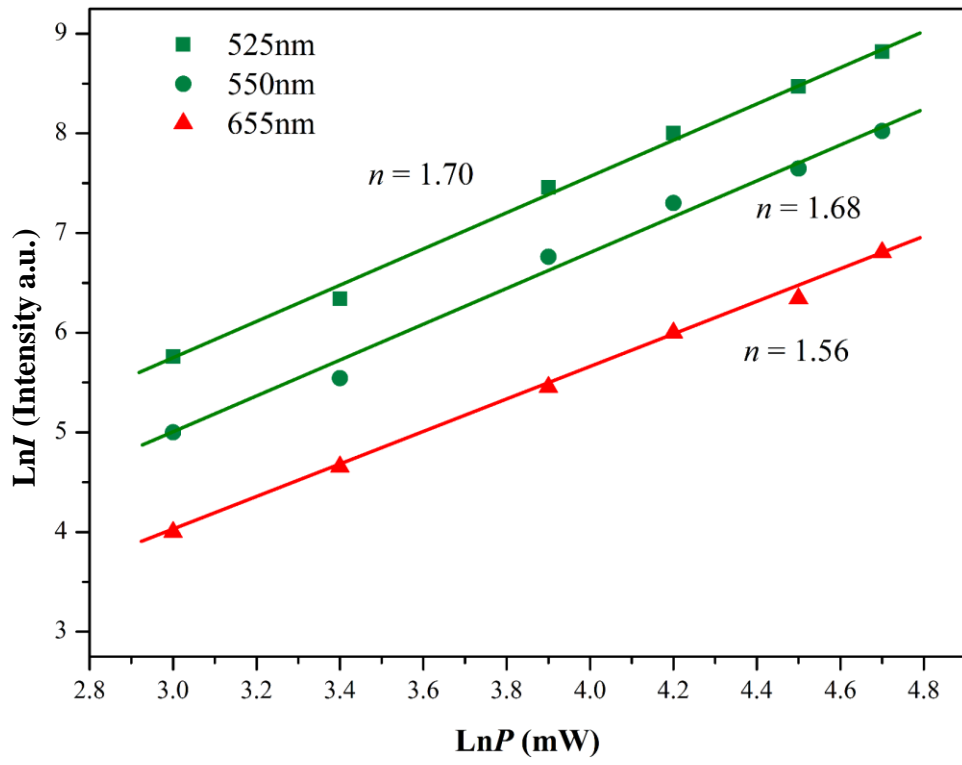
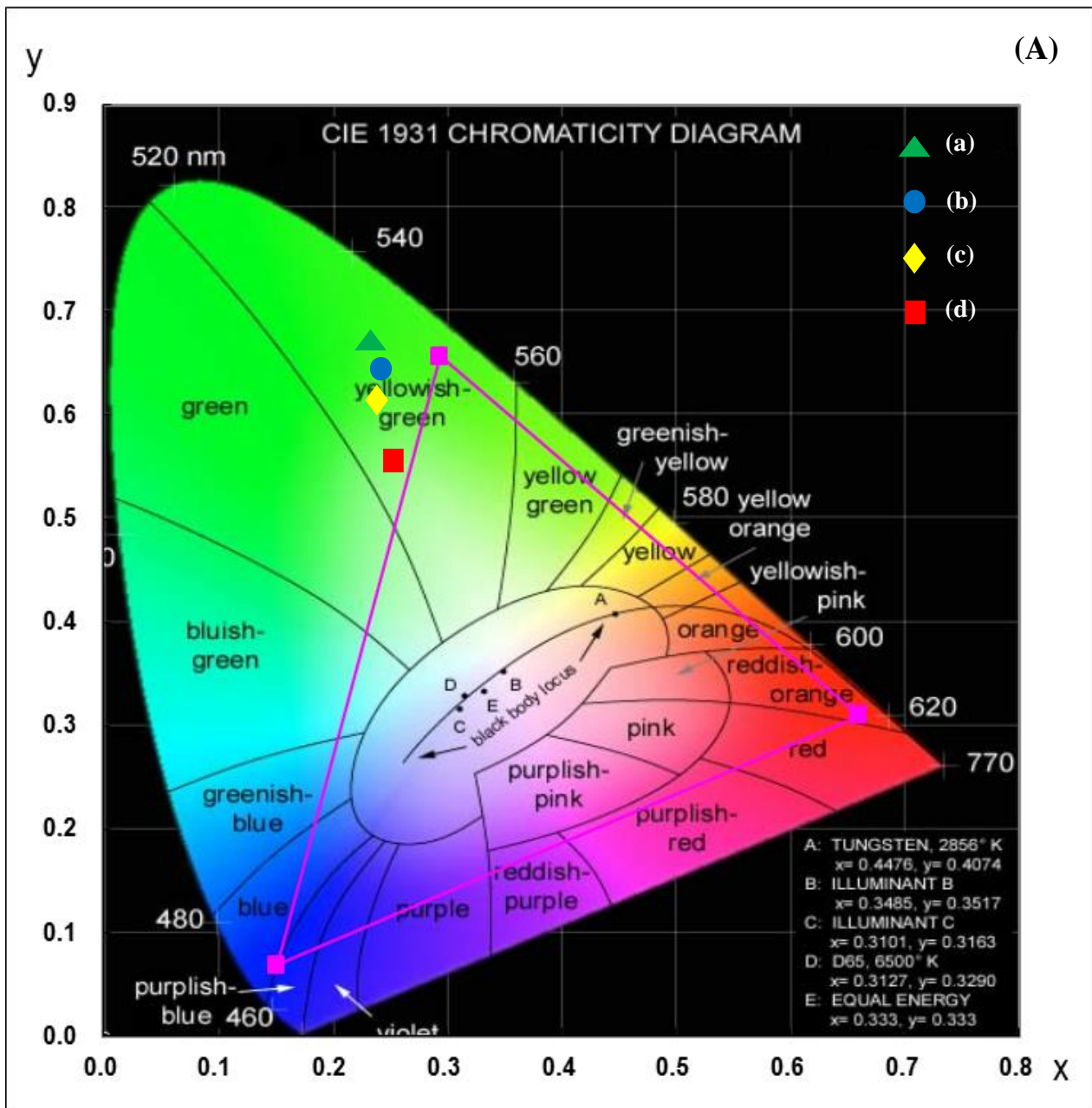


Fig. 8.



(B)

(a)	
x	y
0.237	0.669
(b)	
x	y
0.246	0.640
(c)	
x	y
0.248	0.610
(d)	
x	y
0.269	0.529

Fig. 9.

Supporting Information

Microwave synthesis, microstructural and spectroscopic properties of scheelite-type ternary molybdate upconversion phosphor $\text{NaPbLa}(\text{MoO}_4)_3:\text{Er}^{3+}/\text{Yb}^{3+}$

Chang Sung Lim¹, Aleksandr S. Aleksandrovsky^{2,3}, Victor V. Atuchin^{4,5,6,7}, Maxim S.

Molokeev^{8,9,10}, Aleksandr S. Oreshonkov^{9,11}

¹Department of Aerospace Advanced Materials & Chemical Engineering, Hanseo University,
Seosan 356-706, Republic of Korea

²Laboratory of Coherent Optics, Kirensky Institute of Physics Federal Research Center KSC SB
RAS, Krasnoyarsk 660036, Russia

³Institute of Nanotechnology, Spectroscopy and Quantum Chemistry, Siberian Federal University,
Krasnoyarsk 660041, Russia

⁴Laboratory of Optical Materials and Structures, Institute of Semiconductor Physics, SB RAS,
Novosibirsk 630090, Russia

⁵Functional Electronics Laboratory, Tomsk State University, Tomsk 634050, Russia

⁶Laboratory of Single Crystal Growth, South Ural State University, Chelyabinsk 454080, Russia

⁷Research and Development Department, Kemerovo State University, Kemerovo 650000, Russia

⁸Laboratory of Crystal Physics, Kirensky Institute of Physics, Federal Research Center KSC SB
RAS, Krasnoyarsk 660036, Russia

⁹Siberian Federal University, Krasnoyarsk 660041, Russia

¹⁰Department of Physics, Far Eastern State Transport University, Khabarovsk 680021, Russia

¹¹Laboratory of Molecular Spectroscopy, Kirensky Institute of Physics Federal Research Center
KSC SB RAS, Krasnoyarsk 660036, Russia

Table S1. Fractional atomic coordinates and isotropic displacement parameters (\AA^2) of the $\text{NaPbLa}_{1-x-y}\text{MoO}_4:x\text{Er},y\text{Yb}$ samples

	x	y	z	B_{iso}	Occ.
NPLM					
Na	0	1/4	5/8	0.6 (5)	1/3
Pb	0	1/4	5/8	0.6 (5)	1/3
La	0	1/4	5/8	0.6 (5)	1/3
Mo	0	1/4	1/8	0.5 (5)	1
O	0.231 (3)	0.112 (2)	0.039 (1)	0.5 (7)	1
NPLM:0.05Er,0.35Yb					
Na	0	1/4	5/8	0.6 (4)	1/3
Pb	0	1/4	5/8	0.6 (4)	1/3
La	0	1/4	5/8	0.6 (4)	0.2
Er	0	1/4	5/8	0.6 (4)	0.01666667
Yb	0	1/4	5/8	0.6 (4)	0.11666667
Mo	0	1/4	1/8	1.8 (4)	1
O	0.260 (5)	0.124 (3)	0.065 (2)	3.0 (6)	1
NPLM:0.05Er,0.4Yb					
Na	0	1/4	5/8	0.4 (5)	1/3
Pb	0	1/4	5/8	0.4 (5)	1/3
La	0	1/4	5/8	0.4 (5)	0.18333333
Er	0	1/4	5/8	0.4 (5)	0.01666667
Yb	0	1/4	5/8	0.4 (5)	0.13333333
Mo	0	1/4	1/8	0.8 (5)	1
O	0.271 (4)	0.122 (2)	0.052 (2)	0.5 (6)	1
NPLM:0.05Er,0.45Yb					
Na	0	1/4	5/8	0.4 (5)	1/3
Pb	0	1/4	5/8	0.4 (5)	1/3
La	0	1/4	5/8	0.4 (5)	0.16666667
Er	0	1/4	5/8	0.4 (5)	0.01666667
Yb	0	1/4	5/8	0.4 (5)	0.15
Mo	0	1/4	1/8	1.0 (5)	1
O	0.239 (3)	0.112 (2)	0.047 (1)	0.5 (6)	1
NPLM:0.05Er,0.5Yb					

Na	0	1/4	5/8	0.2 (4)	1/3
Pb	0	1/4	5/8	0.2 (4)	1/3
La	0	1/4	5/8	0.2 (4)	0.15
Er	0	1/4	5/8	0.2 (4)	0.01666667
Yb	0	1/4	5/8	0.2 (4)	0.1666667
Mo	0	1/4	1/8	0.5 (4)	1
O	0.249 (3)	0.111 (2)	0.043 (1)	0.5 (6)	1

Table S2. Main bond lengths (Å) of the NaPbLa_{1-x-y}MoO₄:xEr,yYb samples

NPLM			
(Na/Pb/La)—O ⁱ	2.63 (2)	Mo—O	1.77 (2)
(Na/Pb/La)—O ⁱⁱ	2.53 (2)		
NPLM:0.05Ho,0.35Yb			
(Na/Pb/La/Er/Yb)—O ⁱ	2.47 (2)	Mo—O	1.70 (2)
(Na/Pb/La/Er/Yb)—O ⁱⁱ	2.66 (2)		
NPLM:0.05Ho,0.4Yb			
(Na/Pb/La/Er/Yb)—O ⁱ	2.48 (2)	Mo—O	1.81 (2)
(Na/Pb/La/Er/Yb)—O ⁱⁱ	2.50 (2)		
NPLM:0.05Ho,0.45Yb			
(Na/Pb/La/Er/Yb)—O ⁱ	2.55 (1)	Mo—O	1.73 (1)
(Na/Pb/La/Er/Yb)—O ⁱⁱ	2.55 (1)		
NPLM:0.05Ho,0.5Yb			
(Na/Pb/La/Er/Yb)—O ⁱ	2.53 (1)	Mo—O	1.79 (1)
(Na/Pb/La/Er/Yb)—O ⁱⁱ	2.49 (1)		

Symmetry codes: (i) $-x+1/2, -y, z+1/2$; (ii) $-x+1/2, -y+1/2, -z+1/2$.

Table S3. Cell volume values of scheelite-type molybdates

Compound	Cell volume V, Å ³	Reference
BaMoO ₄	404.912	[45]
PbMoO ₄	357.50	[44]
SrMoO ₄	351.463	[46]
EuMoO ₄	347.75	[47]
NaLa(MoO ₄) ₂	335.01	[48]
NaPbLa(MoO ₄) ₃	342.647	Present work
NaPbLa(MoO ₄) ₃ : 0.05Er ³⁺ , 0.35Yb ³⁺	333.994	Present work
NaPbLa(MoO ₄) ₃ : 0.05Er ³⁺ , 0.4Yb ³⁺	332.036	Present work
NaPbLa(MoO ₄) ₃ : 0.05Er ³⁺ , 0.45Yb ³⁺	331.056	Present work
NaPbLa(MoO ₄) ₃ : 0.05Er ³⁺ , 0.45Yb ³⁺	329.911	Present work
NaSrLa(MoO ₄) ₃	339.84	[29]
NaSrLa(MoO ₄) ₃ : 0.2Er ³⁺	335.9	[29]
NaSrLa(MoO ₄) ₃ : 0.1Er ³⁺ , 0.2Yb ³⁺	333.65	[29]
NaSrLa(MoO ₄) ₃ : 0.05Er ³⁺ , 0.45Yb ³⁺	328.92	[29]
NaCaLa(MoO ₄) ₃	326.366	[28]
NaCaLa(MoO ₄) ₃ : 0.2Er ³⁺	322.687	[28]
NaCaLa(MoO ₄) ₃ : 0.1Er ³⁺ , 0.2Yb ³⁺	320.086	[28]
NaCaLa(MoO ₄) ₃ : 0.05Er ³⁺ , 0.45Yb ³⁺	315.177	[28]
CaMoO ₄	311.552	[49]
NaCaGd(MoO ₄) ₃	312.304	[50]
NaCaGd(MoO ₄) ₃ : 0.2Er ³⁺	311.263	[50]
NaCaGd(MoO ₄) ₃ : 0.1Er ³⁺ , 0.2Yb ³⁺	310.02	[50]
NaCaGd(MoO ₄) ₃ : 0.05Er ³⁺ , 0.45Yb ³⁺	308.075	[50]
CdMoO ₄	297.6	[24]

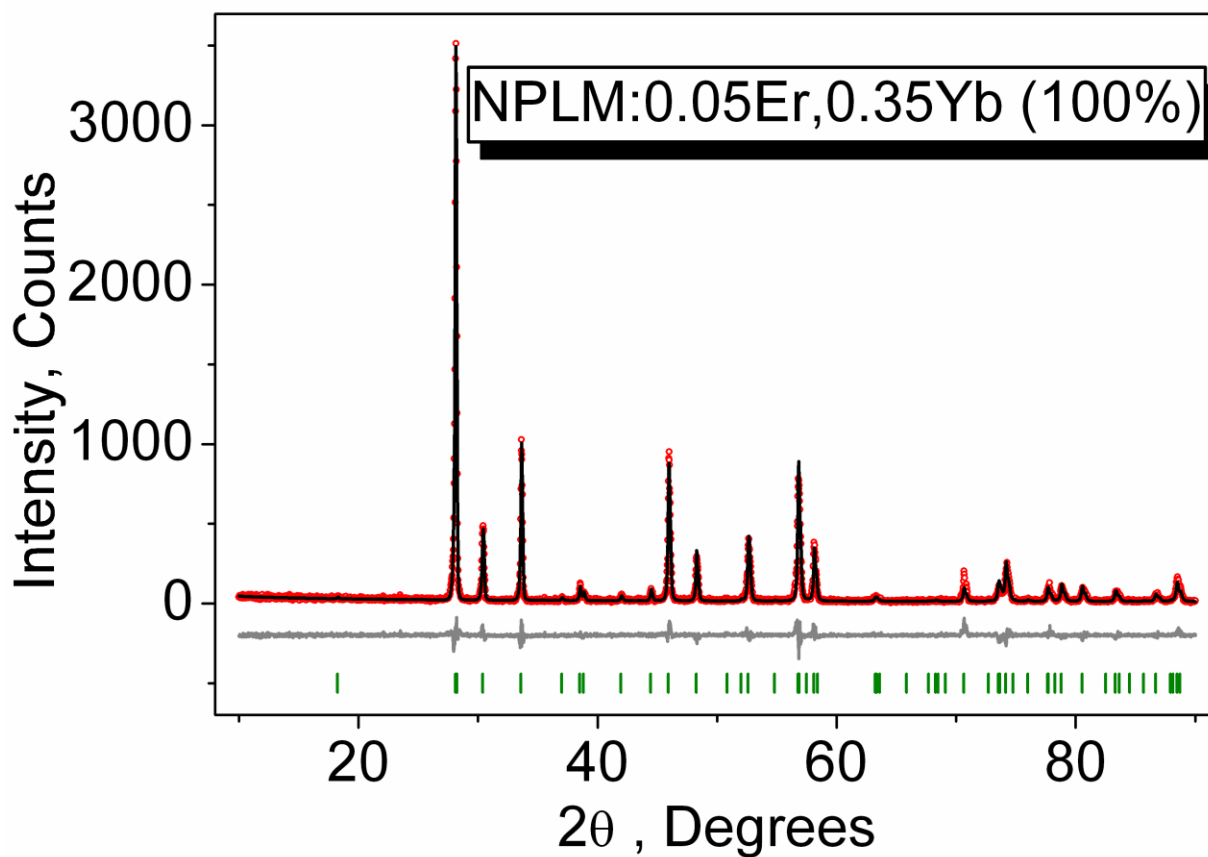


Figure S1. Difference Rietveld plot of NPLM:0.05Er,0.35Yb

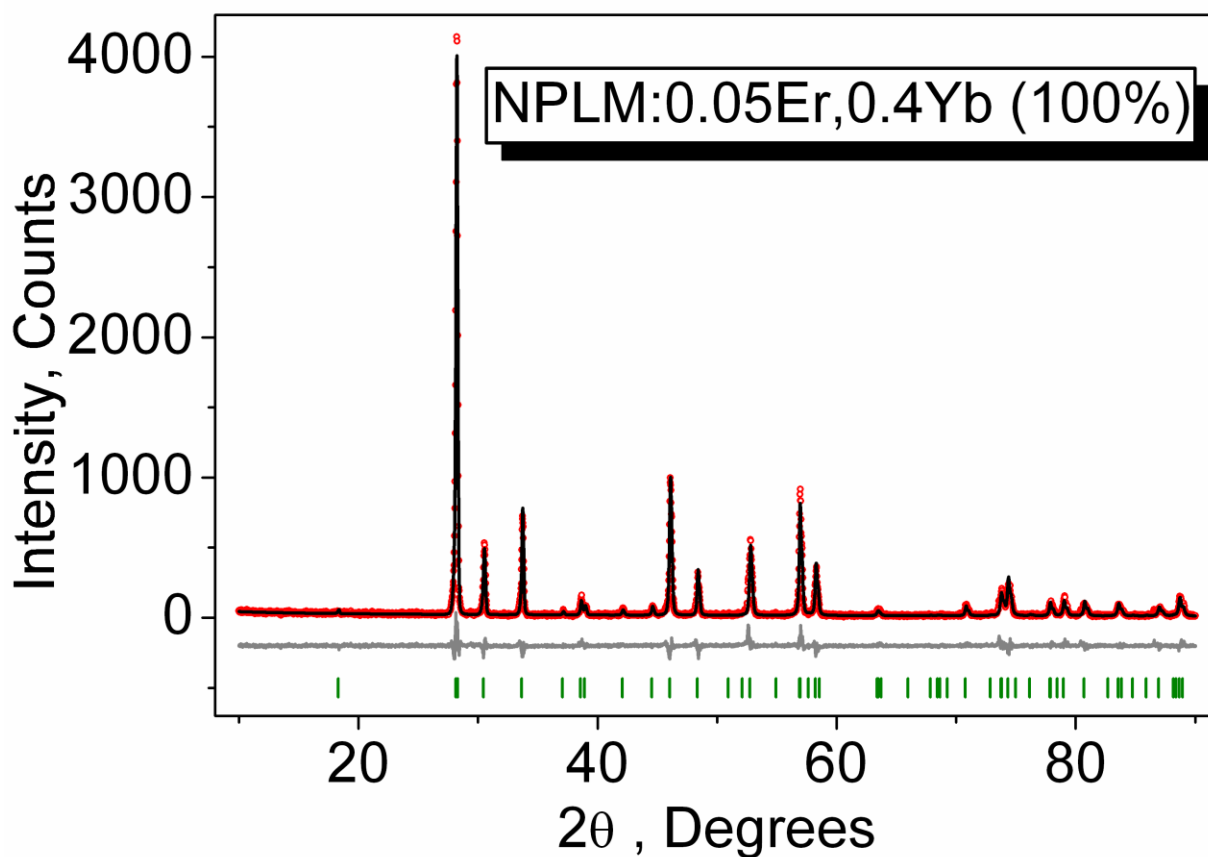


Figure S2. Difference Rietveld plot of NPLM:0.05Er,0.4Yb

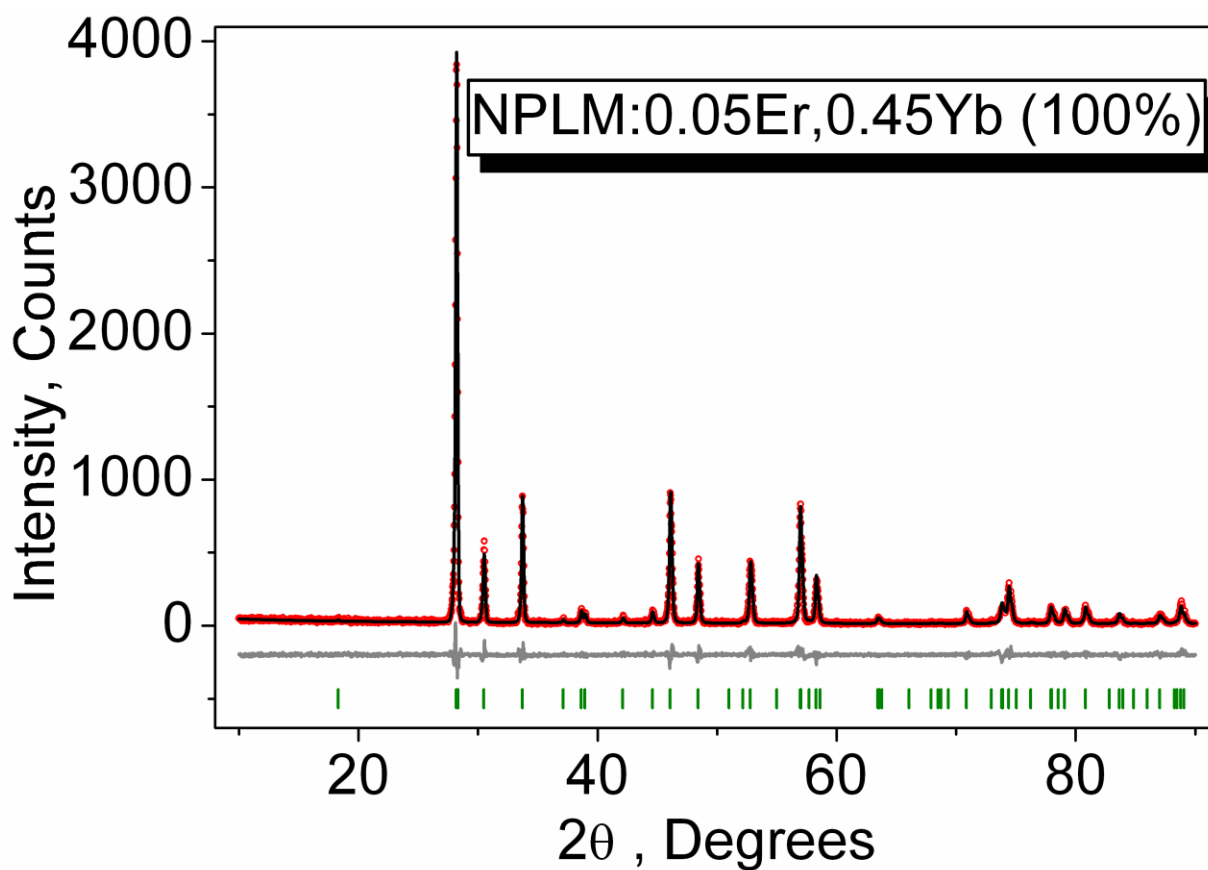


Figure S3. Difference Rietveld plot of NPLM:0.05Er,0.45Yb

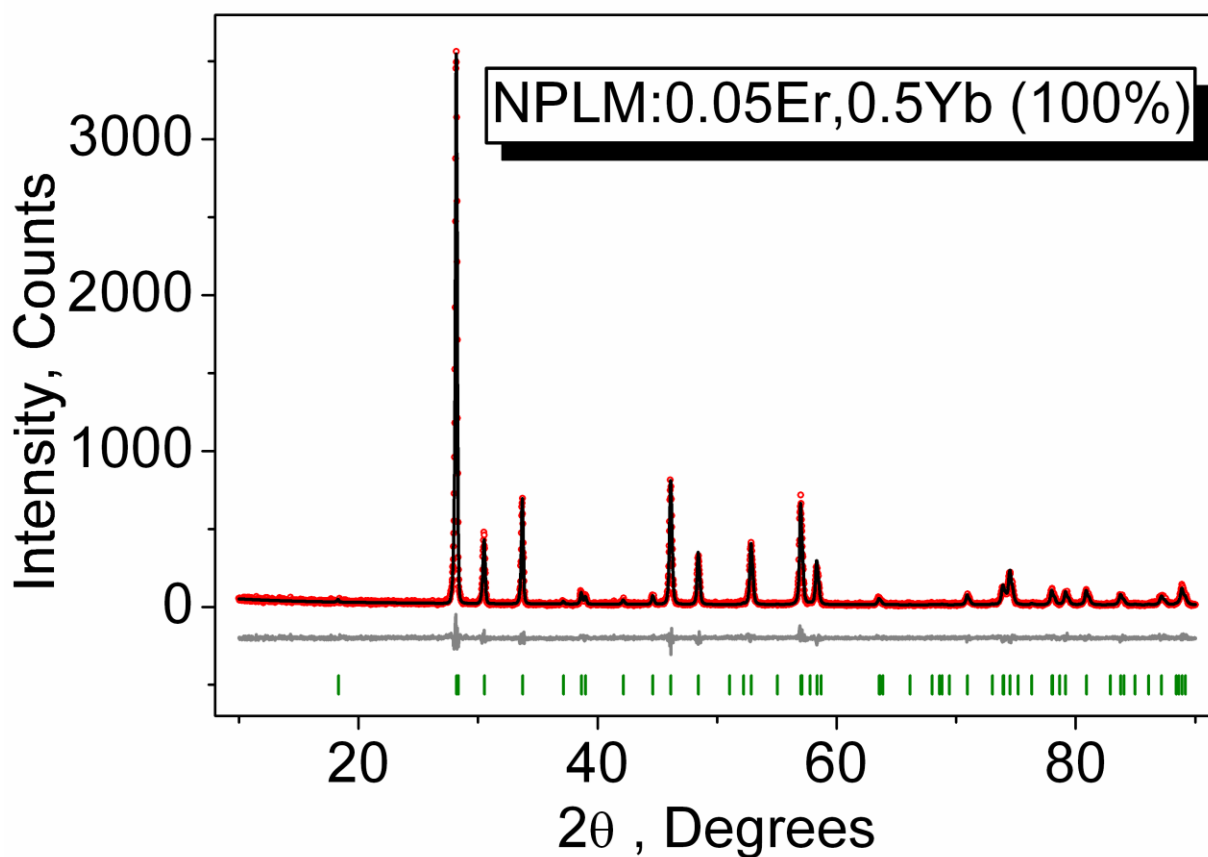


Figure S4. Difference Rietveld plot of NPLM:0.05Er,0.5Yb

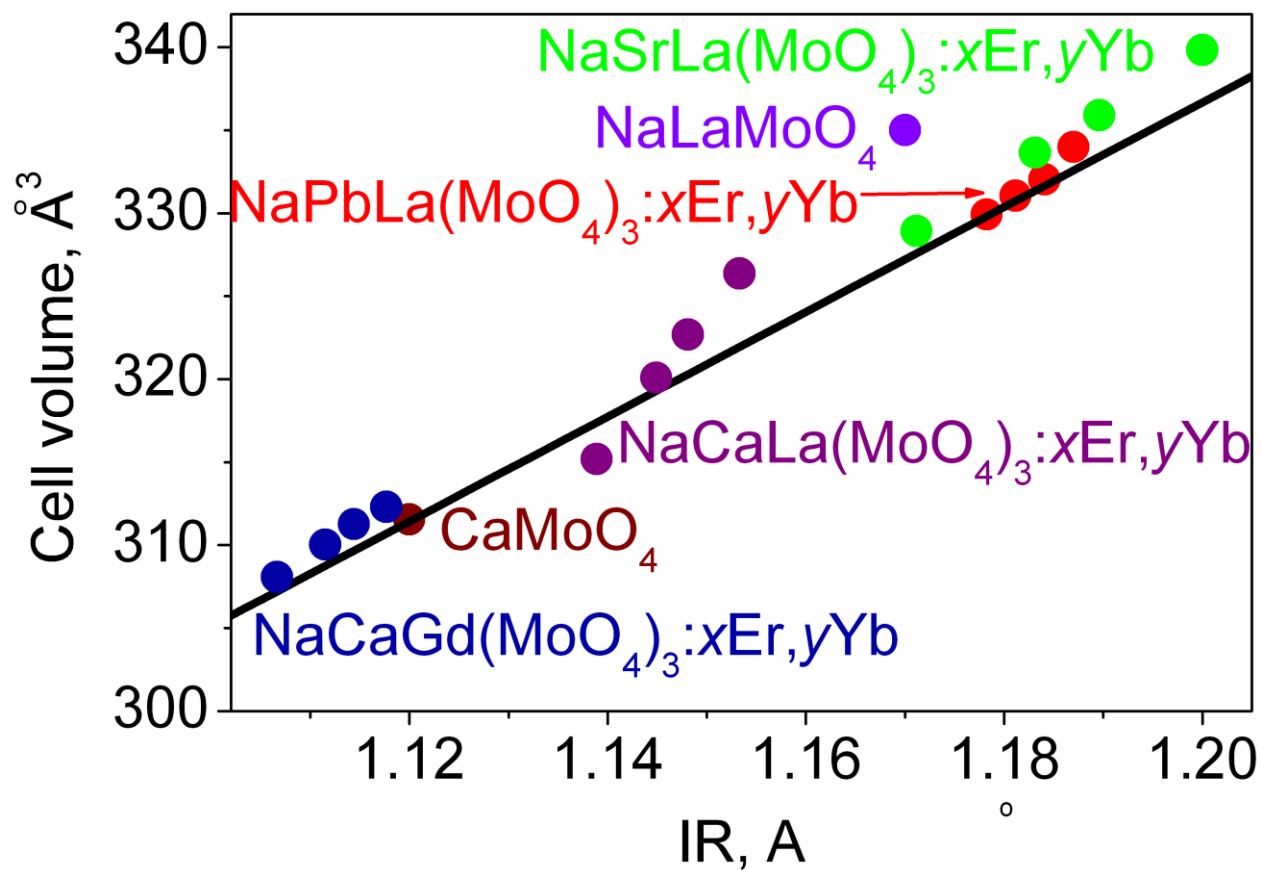


Figure S5. Dependence of cell volume on averaged big ion radii IR in known ternary scheelite-type molybdates.